Numerical simulation of laser propagation in atmosphere and an adaptive optics system in static state

Hai-Xing Yan*, Shu-Shan Li, De-Liang Zhang, and She Chen

(Institute of Mechanics, Chinese Academy of Sciences, Beijing 100080, China)

ABSTRACT

A comprehensive model of laser propagation in atmosphere and all portions of an adaptive optics (AO) system for phase compensation is presented and the corresponding computer program is compiled. By using the direct wavefront gradient control method to reconstruct the wavefront phase and utilizing the long-exposure Strehl ratio as the evaluation parameter, the numerical simulation of an AO system in static state with atmospheric propagation of laser beam is carried out. It is found that on certain conditions the phase-screen which describes turbulence in the atmosphere might not be isotropic. The numerical experiments show that the computational results in imaging of lenses by means of the fast Fourier transform (FFT) method agree excellently with those by means of integration method. However, the computer time of FFT method is one order of magnitude less than that of integration method. We present "phase tailoring" of the calculated phase to solve the problem that variance of the calculated residual phase does not correspond to the correction effectiveness of an AO system. It is found for the first time that for a constant delay time of the AO system, when the lateral wind speed exceeds a threshold, the compensation effectiveness of an AO system is better than that of complete phase conjugation. It indicates that a better compensation capability of an AO system does not mean a better correction effectiveness.

Keywords: Adaptive optics system, Laser propagation in atmosphere, Numerical simulation, Phase compensation, Wavefront reconstruction

1. INTRODUCTION

It is well known that the turbulent atmosphere deteriorates the optical wave which propagates in the atmosphere. Astronomical observation and laser propagation are the most important fields which are related to this problem. An adaptive optics (AO) system can be used to partially overcome the atmospheric deterioration of the optical wave.[1] Generally, an AO system can be divided into three portions: wavefront detection, wavefront reconstruction and wavefront correction. A Hartmann-Shack detector is used to do a real-time detection of the deformed wavefront. The widely-used wavefront reconstruction methods are the direct wavefront gradient control method[2,3] and the modal wavefront reconstruction method in terms of Zernike polynomials expansion.[4] A deformable mirror is often used to correct the wavefront.

A theoretical model and numerical computation can be used to simulate the propagation of optical wave in the turbulent atmosphere and operation of an AO system. In this way, one can design a new AO system, estimate its performances and compare the different scheme to obtain the optimum choice. Furthermore, one can do numerical experiments for an existing AO system to investigate its operation and performances to get some valuable knowledge. It is possible and convenient for the numerical simulation to operate the system on a great deal of different conditions some of which might not easily and/or impossibly realize in a real experiment.

In the field of numerical simulation of optical wave propagation in the turbulent atmosphere, Fleck and his colleagues utilized the multiple phase-screen method to calculate the three-dimensional laser beam propagation numerically.[5] Flatte et al utilized the similar approach to investigate the intensity and statistics by means of numerical simulation of wave propagation in 3-D random media.[6]

In the field of theoretical investigation of an AO system, most investigators utilize the analytically theoretical analyses to simulate the AO system, calculate its performances and get some insights into it. They have published a great deal of articles in this respect, for example, see [7,8]. A few investigators utilized the numerical simulation to calculate and investigate the performances of an AO system. They published some articles in proceedings (for example, see [9]). However, the detailed theoretical model and computational results were not included in these articles (for example, see [10,11]).

* Correspondence: Email: hxyan@imech.ac.cn; Telephone: (86) 10 62545533 ext. 2138; Fax: (86) 10 62561284

Part of the SPIE Conference on Propagation and Imaging through the Atmosphere III • Denver, Colorado • July 1999
SPIE Vol. 3763 • 0277-786X/99/$10.00

We have been pursuing the numerical simulation of atmospheric propagation of laser beam and an AO system since 1988. This is the first time for us to publish an article in an international symposium. We utilize numerical simulation to get some insights into the atmospheric propagation of optical wave and an AO system. A comprehensive theoretical model was presented and the corresponding computer program was compiled. Both of the atmospheric propagation of optical wave and the operation of an AO system were included in it. We took the laser beam propagated in the atmosphere with an active AO system as an example. Simulating the operation of a real AO system, a laser beam from a beacon propagates through a turbulent media to obtain the deformed wavefront, then the deformed wavefront is detected, reconstructed and corrected by the AO system. Finally, a phase-compensated beam from the main laser propagates in the same but moved (because of the time delay in the AO system and actions of the lateral wind speed and/or lateral movements of target and main laser) turbulent media again to reach the target. The long-exposure Strehl ratio is used to evaluate the performances of the AO system.

This article is characterized mainly in that (1) it is a "pure" numerical simulation of the propagation of optical wave in a turbulent media and an AO system. (2) The numerical simulation of the propagation of optical wave in a turbulent media and the numerical simulation of all portions of an AO system are combined. The turbulence-deformed wavefront phase is used as the object of treatment of the AO system and the optical wave with compensated wavefront phase propagates in the same turbulent media. (3) The various conditions in the practical applications of wave propagation and AO system can be included in an exactly similar way.

2. THEORETICAL MODEL AND NUMERICAL SIMULATION OF LASER PROPAGATION IN TURBULENT MEDIA

In the case of optical wave propagation to the forward (z) direction, the Maxwell wave equation in the parabolic or Fresnel approximation can be rewritten as

$$2ik\frac{\partial\varphi}{\partial z}+\frac{\partial^2\varphi}{\partial x^2}+\frac{\partial^2\varphi}{\partial y^2}+k^2(n^2-n_0^2)\varphi=0, \tag{1}$$

where

$$\varphi(x,y,z)=E(x.y,z)\exp(-ikz), \tag{2}$$

$E(x,y,z)$ is a slowly varying wave field amplitude, wavenumber $k=2\pi/\lambda$, n is the refractive index, n_0 is the refractive index in the media without turbulence, in the atmosphereic propagation n_0 can be taken as 1 and

$$n^2-n_0^2=(n_0-n_1)^2-n_0^2\approx 2n_1, \tag{3}$$

$n_1=n-n_0$ is the deviation of the refractive index which is a stochastic quantity.

In the case of laser beam propagation, a focused beam is quite important and common. For the focused beam, we utilize the following coordinate transformations

$$\begin{cases}\bar{x}=x/[a(1-z/l)]\\ \bar{y}=y/[a(1-z/l)]\\ \zeta=z/(ka^2)\end{cases} \tag{4}$$

where a is the radius of the beam, l is the transformation factor, $l>0$ correspands to a convergent beam, $l<0$ correspands to a divergent beam, and $l\to\infty$ correspands to a parallel beam.

The propagation equation (1) can be accordingly changed into:

$$2i\frac{\partial\psi}{\partial\zeta}+\frac{1}{(1-ka^2\zeta/l)^2}\left(\frac{\partial^2\psi}{\partial\bar{x}^2}+\frac{\partial^2\psi}{\partial\bar{y}^2}\right)+2k^2a^2n_1\psi=0, \tag{5}$$

where

$$\psi(\bar{x},\bar{y},\zeta)=\sqrt{\frac{ca^2}{8\pi P_T}}(1-z/l)\varphi(x.y,z)\exp\left[\frac{ik(x^2+y^2)}{2l(1-z/l)}\right], \tag{6}$$

P_T is the total beam power, c is the light speed. We utilize Eq.(5) as the basic propagation equation in the numerical simulation. It is changed into a difference equation and solved numerically.

Similar to Fleck et al,[5] we utilize the multiple phase screen model to describe the turbulent media. Its main idea is as following. The effects of turbulence on the optical wave are in terms of the random change of refractive index n_1. The turbulent media can be divided into several segments which may have different lengths although we utilize the equally spaced segments for sake of simplicity. It is thought that each segment can deform phase of the optical wave independently which propagates in it and does not have a practical influence on the amplitude of the wave. The amplitude of optical wave is changed in the propagation process of the wave with deformed phase. It means that we can treat the changes of amplitude and phase of optical wave separately. Thus, the contribution of the turbulent media segment to the phase of optical wave can be "pressed" into a very thin phase screen and add to the initial phase of the wave. Then, the wave with changed phase propagates to reach the next phase screen in a media without turbulence. At the position of next phase screen, the wave with changed amplitude is added the contribution of the new phase screen and so on. This process continues until the wave reaches the target.

The effect of a turbulent media segment on the optical wave phase can be deduced as following. In the propagation equation (5), remove the terms of diffraction and get

$$2i\frac{\partial \psi}{\partial \zeta} + 2k^2 a^2 n_1 \psi = 0 \cdot \tag{7}$$

Its solution is

$$\psi(\bar{x},\bar{y},\zeta+\Delta\zeta) = \psi(\bar{x},\bar{y},\zeta)\exp(ik^2a^2n_1\Delta\zeta) = \psi(\bar{x},\bar{y},\zeta)\exp(ikn_1\Delta z), \tag{8}$$

where $\Delta z = ka^2\Delta\zeta$ is the step length in z direction in calculating the turbulent effect. It means that the effect of turbulent media segment is equivalent to adding an additional phase $n_1\Delta z$ to initial phase of the optical wave. In the practical calculation, it is assumed that the additional phase is added in an unlimitedly thin "phase screen", i.e.

$$\psi(\bar{x},\bar{y},\zeta^+) = \psi(\bar{x},\bar{y},\zeta)\exp(ikn_1\Delta z) \cdot \tag{9}$$

Then, the wave field $\psi(\bar{x},\bar{y},\zeta^+)$ propagates to reach the next phase screen in a media without turbulence to obtain $\psi(\bar{x},\bar{y},\zeta+\Delta\zeta)$. Now the remain problem is to obtain the additional phase $\Gamma(x,y)$ of a turbulent media segment Δz.

It can be proved that in the difference form

$$\begin{aligned}\Gamma(x,y) &= n_1\Delta z \\ &= (\pi\Delta z\Delta k_x\Delta k_y)^{1/2}\sum_{I=-\frac{N_x}{2}+1}^{\frac{N_x}{2}}\sum_{J=-\frac{N_y}{2}+1}^{\frac{N_y}{2}}\exp(iI\Delta k_x x + iJ\Delta k_y y)\Phi_n^{\frac{1}{2}}(I\Delta k_x, J\Delta k_y) \\ &\cdot[a_1(I\Delta k_x, J\Delta k_y) + ia_2(I\Delta k_x, J\Delta k_y)]\end{aligned} \tag{10}$$

where $\Phi_n(k_x,k_y) = \Phi_n(k_x,k_y,0)$ is the spectral density for the refractive index fluctuations. We make the usual assumption of a von Karman spectrum, which specifies that

$$\Phi_n(k_x,k_y) = 0.033C_n^2(k_0^2 + k_x^2 + k_y^2)^{-11/6}, \tag{11}$$

here C_n^2 is the index structure constant and $k_0 = 2\pi/L_0$, where L_0 is the outer scale length of the turbulence. In deducing process, $\Delta z >> L_0$ is required. a_1 and a_2 are two-dimensional complex random numbers. These independent random numbers are assumed to obey Gaussian statistics and to have variance 1. Furthermore, it is required that

$$\begin{aligned}a_1(k_x,k_y) &= a_1(-k_x,-k_y) \\ a_2(k_x,k_y) &= -a_2(-k_x,-k_y)\end{aligned} \tag{12}$$

The step lengths Δk_x and Δk_y of wavenumbers k_x and k_y are

$$\begin{aligned}\Delta k_x &= \frac{2\pi}{N_x\Delta x} = \frac{2\pi}{N_x\Delta\bar{x}a(1-ka^2\zeta/l)} \\ \Delta k_y &= \frac{2\pi}{N_y\Delta y} = \frac{2\pi}{N_y\Delta\bar{y}a(1-ka^2\zeta/l)}\end{aligned} \tag{13}$$

where N_x, N_y are the grid numbers in x, y direction and $\Delta x, \Delta y$ are the corresponding step lengths, respectively.

Combining Eqs.(10)-(13), $\Gamma(x,y)$ can be calculated from the double sum (assuming the grid numbers $N_x = N_y = N$)

$$\Gamma(m_x\Delta x, m_y\Delta y) = \frac{2\pi}{N}\left(\frac{0.033\pi\Delta z C_n^2}{\Delta x\Delta y}\right)^{1/2} \sum_{I=-\frac{N}{2}+1}^{\frac{N}{2}} \sum_{J=-\frac{N}{2}+1}^{\frac{N}{2}} \frac{\exp\left(\frac{2\pi I i m_x}{N} + \frac{2\pi J i m_y}{N}\right)}{\left[\left(\frac{2\pi}{L_0}\right)^2 + \left(\frac{2\pi I}{N\Delta x}\right)^2 + \left(\frac{2\pi J}{N\Delta y}\right)^2\right]^{11/12}} \cdot [a_1(I\Delta k_x, J\Delta k_y) + i a_2(I\Delta k_x, J\Delta k_y)] \tag{14}$$

which can be computed by a sequence of FFT operations.

3. THEORETICAL MODEL AND NUMERICAL SIMULATION OF AN AO SYSTEM

This article only includes the simulation of an AO system in the static state. In a practical AO system, the dynamic control process must be included to make the system to work stably. As the first stage, we ignore the dynamic control process in this article. It is well known that an AO system must have a time delay because the system has a limited response and all the wavefront detection, reconstruction and correction have to take some time in practice. We treat the effects of the time delay in this article as following. Based on the well-known Taylor assumption, the turbulence (i.e. the phase screens) is considered to be "frozen" in a short time period (for example, within a few ms). The phase screens are considered to move laterally in the delay time period under the actions of lateral wind and/or the lateral movements of laser source and target. Thus, the laser beam with compensated phase will propagate in the laterally moved phase screens to reach the target with a deteriorated correction effect (see Fig. 1). The phase reconstruction in this article is based on the direct wavefront gradient control method.[2,3] The effects of noise and detection errors in an AO system are ignored in this article as well.

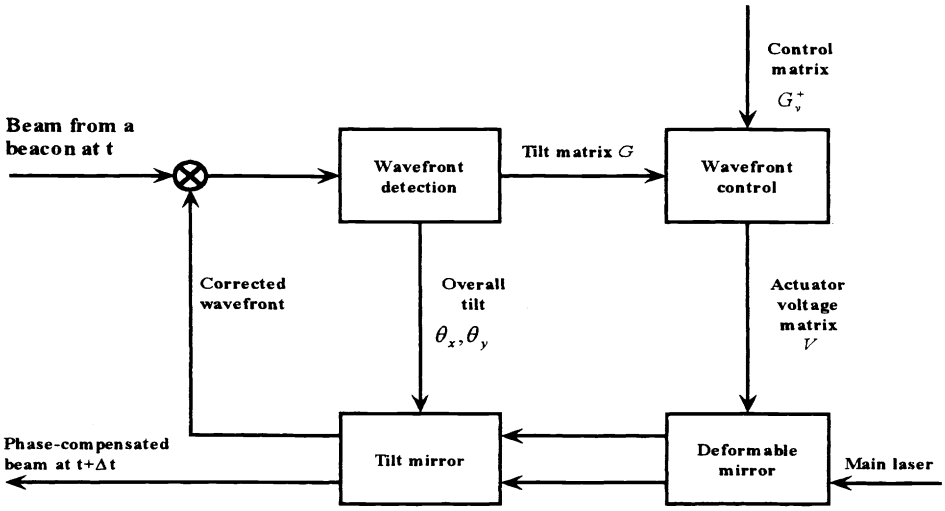

Fig.1 Combination of the numerical simulation of the laser propagation in atmosphere with that of an AO system

3.1. Wavefront Detection

The wave field of the beam which radiates from a beacon propagates through a turbulent media and arrives a Hartmann-Shack (HS) detector. The detector is divided into several sub-apertures according to the practical arrangement. The wave field of a sub-aperture $u_1(x_0, y_0)$ propagates to reach the focus plane of HS detector. Its wave field becomes

$$u_2(x,y) = \iint_\Sigma \frac{f}{j\lambda r^2} e^{jkr} u_1(x_0, y_0) dx_0 dy_0, \tag{15}$$

where $\iint_\Sigma$ expresses the integral on the sub-aperture, r is the distance between point (x,y) on the focus plane and point (x_0, y_0) on the sub-aperture. The position of the optical center can be calculated as

$$x_c = \iint_T x|u_2(x,y)|^2 dxdy \Big/ \iint_T |u_2(x,y)|^2 dxdy, \tag{16}$$

$$y_c = \iint_T y|u_2(x,y)|^2 dxdy \Big/ \iint_T |u_2(x,y)|^2 dxdy, \tag{17}$$

where $\iint_T$ expresses the integral on the focus plane. Further, taking the position of optical center of focused plane wave field of the sub-aperture as 0, the average tilts of the sub-aperture in the x and y directions can be calculated as

$$G_x = \frac{2\pi}{f\lambda} x_c, \tag{18}$$

$$G_y = \frac{2\pi}{f\lambda} y_c, \tag{19}$$

where f is the focus length of the sub-aperture.

In a practical AO system, the overall tilt of the wavefront is corrected by a specific tilt correction mirror. In our numerical simulation, we separate the overall tilts in the x and y directions as

$$\theta_x = \frac{1}{m}\sum_{i=1}^{m} G_x(i), \tag{20}$$

$$\theta_y = \frac{1}{m}\sum_{i=1}^{m} G_y(i), \tag{21}$$

where m is the number of sub-apertures, $G_x(i)$ and $G_y(i)$ are the average tilts of the i-th sub-aperture in x and y directions, respectively. The average tilts of each sub-aperture after subtracting the overall tilts in x and y directions constitute the tilt matrix G. In this article, it is assumed that the tilt correction mirror can completely correct the overall tilt θ_x and θ_y.

3.2. Wavefront Reconstruction

The main task of wavefront reconstruction is to obtain the control matrix. The control matrix multiplies the tilt matrix G to get the actuator voltage matrix V.

Now, we deduce the control matrix by utilizing the direct wavefront gradient control method. The surface shape of deformable mirror that is the corrected wavefront itself can be expressed as

$$\psi_m(x,y) = \sum_{j=1}^{K} V_j R_j(x,y), \tag{22}$$

where K is the total number of actuators of the deformable mirror, V_j is the voltage of j-th actuator, $R_j(x,y)$ is the influence function of j-th actuator which describes the effect of unit displacement of j-th actuator on the surface shape of the deformable mirror. In principle, the influence function of each actuator may be different and this effect can be included in our numerical simulation. However, in present article it is assumed that all actuators of the deformable mirror have same Gaussian influence function:

$$R_j(x,y) = \frac{2\pi}{\lambda} e^{\ln b\left[(x-x_j)^2+(y-y_j)^2\right]/d^2}, \tag{23}$$

where b is the coupling factor between the adjacent actuators, x_j and y_j are the coordinates of j-th actuator and d is the distance between the adjacent actuators. In fact, any type influence function of the actuator can be used in our simulation computation.

Differentiating the corrected wavefront $\psi_m(x,y)$ with respect to x and y and taking averaging on the sub-aperture, it can be deduced that

$$G_{xi} = \sum_{j=1}^{K} G_{vxij} V_j, \tag{24}$$

$$G_{yi} = \sum_{j=1}^{K} G_{vyij} V_j, \tag{25}$$

where

$$G_{vxij} = \frac{1}{s_i}\iint_{S_i} \frac{\partial R_j(x,y)}{\partial x} dxdy, \tag{26}$$

$$G_{vyij} = \frac{1}{s_i}\iint_{S_i} \frac{\partial R_j(x,y)}{\partial y} dxdy, \tag{27}$$

here $\iint_{S_i}$ is the integral on i-th sub-aperture, S_i is the area of i-th sub-aperture. G_{vxij} and G_{vyij} can be considered as the average tilts on i-th sub-aperture produced by unit displacement of j-th actuator. Expressing by matrix, it becomes

$$G = G_v V. \tag{28}$$

Eq.(28) can be solved in terms of the least square method to obtain

$$V = G_v^+ G, \tag{29}$$

where G_v^+ is the generalized inverse matrix with least-square and minimum norm of matrix G_v. G_v^+ can be deduced by decomposition of singular values. G_v^+ is the control matrix of the direct gradient control wavefront reconstruction.

3.3. Wavefront Correction

In a practical AO system, the wavefront correction is realized by a high speed tilt correction mirror and a deformable mirror. Correspondingly, the corrected wavefront phase of the main laser beam can be expressed as

$$\psi_c = \psi_{tilt} + \psi_m = \theta_x x + \theta_y y + \sum_{j=1}^{K} V_j R_j(x, y). \tag{30}$$

4. RESULT AND DISCUSSION

Strehl ratio is a very useful parameter to describe the propagation quality of optical wave. We utilize six Strehl ratios in our numerical simulation. The ratio of the brightnesses of the brightest point on the target after propagating in the turbulent media and in vacuum in the same condition is defined as STRA. The ratio of the optical energies within a circle around the brightest point having a radius of the first dark ring in the Airy pattern after propagating in the turbulent media and in vacuum is defined as STRAA. STRB and STRBB are the ratios for the center point on the target instead of the brightest point, respectively. STRC and STRCC are the ratios for the optical center on the target, respectively. Similar to the experiment, we utilize long-exposure Strehl ratio which is obtained from the accumulated wave field.

Table 1 Six Strehl ratios

Computational conditions: $\lambda = 0.6328\mu$; L=1km; open loop (OL); $C_n^2 = 10^{-14}\,\mathrm{m}^{-2/3}$; phase screen grids: 512*512; propagation grids: 128*128, center; 10 phase screens.

Times	1	2	3	30	40	50	100	200
STRA	0.0675	0.0480	0.0409	0.0158	0.0145	0.0139	0.0137	0.0132
STRB	0.0154	0.0109	0.0113	0.0089	0.0112	0.0116	0.0119	0.0116
STRC	0.0188	0.0062	0.0139	0.0089	0.0112	0.0116	0.0121	0.0121
STRCC	0.254	0.200	0.210	0.143	0.156	0.157	0.162	0.152
STRBB	0.132	0.121	0.170	0.155	0.162	0.161	0.164	0.163
STRCC	0.225	0.197	0.192	0.155	0.162	0.161	0.164	0.164

Table 1 shows that it is necessary to take averaging by using many times turbulence realizations in order to get relatively stable results and generally, 50 times are enough. It is shown also that the values of long exposure averaged STRA, STRB and STRC are comparable, the values of long exposure averaged STRAA, STRBB and STRCC are comparable, and the former values are much smaller than the latter values.

Table 2 STRCC in different turbulent media

Computational conditions: 61 units AO system; others see Table 1.

C_n^2 ($\mathrm{m}^{-2/3}$)	Times	1	2	3	30	40	50	100	200
$10^{-14.5}$	OL	0.596	0.551	0.492	0.496	0.520	0.514	0.495	0.502
	AO	0.881	0.883	0.876	0.859	0.858	0.858	0.856	0.854
10^{-14}	OL	0.225	0.197	0.192	0.155	0.162	0.161	0.164	0.164
	AO	0.649	0.601	0.585	0.605	0.612	0.616	0.614	0.612
$10^{-13.5}$	OL	0.0978	0.0634	0.0613	0.0536	0.0532	0.0523	0.0487	0.0490
	AO	0.165	0.214	0.210	0.223	0.221	0.220	0.214	0.212

It is found that the relative variances of STRA, STRB and STRC are always larger than those of STRAA, STRBB and STRCC. It means fluctuations of STRA, STRB and STRC are larger than those of STRAA, STRBB and STRCC. We choose STRCC as the evaluation parameter.

It is shown in Table 2 that in a turbulent media with different strength, 40-50 times realizations generally can give relatively stable averaged Strehl ratio and the Strehl ratio becomes worse rapidly as turbulence is stronger.

Table 3 Effect of grid number of propagation on Strehl ratio

Computational conditions: 50 times realizations; open loop (OL); propagation grids in center; others see Table 1.

C_n^2 ($m^{-2/3}$)	$10^{-13.5}$		10^{-14}		$10^{-14.5}$	
Grid number	128×128	256×256	128×128	256×256	128×128	256×256
STRCC	0.0523	0.0538	0.161	0.193	0.514	0.524

Table 3 shows that the computational results by using grid numbers of 128*128 are comparable to those by using grid numbers of 256*256. However, the computer time by using grid number of 128*128 is only about one fourth of that by using 256*256 grids.

It is found that when utilizing an improper phase screen creation method i.e. an improper random number creation method, it is possible to produce phase screens without isotropism (see Table 4). It is apparent that by using the first kind of phase screen, the averaged Strtehl ratios after passing through the phase screens at different positions in the x direction are comparable. However, it is not the case in the y direction. We checked the independent random numbers $a_1(k_x,k_y)$ and $a_2(k_x,k_y)$ (see Eqs.(10) and (14)) carefully and found that they obey Gaussian statistics and have variance 1. By utilizing another kind of random numbers, the second kind of phase screen was produced. It is shown that this kind of phase screen is perfectly isotropic (see Table 5).

Table 4 Test of isotropism of phase screens (I)

Computational conditions: $\lambda = 0.6328\mu$; L=340m; open loop (OL); $C_n^2 = 2.78*10^{-14}(r_0 = 5cm)$; first kind of phase screen; phase screen grids: 512*512; propagation grids: 128*128; 10 phase screens.

Position	x-grid	y-grid	10 times	20 times	50 times
Left-1	65-192	193-320	0.276	0.285	0.262
Center	193-320	193-320	0.229	0.214	0.238
Right-1	321-448	193-320	0.230	0.181	0.228
Upper-1	193-320	321-448	0.315	0.372	0.362
Center	193-320	193-320	0.229	0.214	0.238
Lower-1	193-320	65-192	0.238	0.210	0.181

Table 5 Test of isotropism of phase screens (II)

Computational conditions: same as Table 1 besides the propagation grid position; second kind of phase screen.

Position	x-grid	y-grid	10 times	20 times	50 times	100 times	200 times
Left-1	65-192	193-320	0.157	0.180	0.183	0.170	0.169
Center	193-320	193-320	0.161	0.166	0.161	0.164	0.164
Right-1	321-448	193-320	0.155	0.165	0.181	0.174	0.175
Upper-1	193-320	321-448	0.205	0.168	0.161	0.165	0.164
Center	193-320	193-320	0.161	0.166	0.161	0.164	0.164
Lower-1	193-320	65-192	0.216	0.198	0.178	0.179	0.167

It is found that in comparison to [5], our coordinate transformations Eq.(4) for focussed beam is profittable in that the positions of the phase screens are not influenced by the coordinate transformations. It is quite easy to arrange equally spaced screens. Another advantage of the coordinate transformations is that it is possible to get comparable results by utilizing less phase screens so that the computer time can be saved (see Table 6).

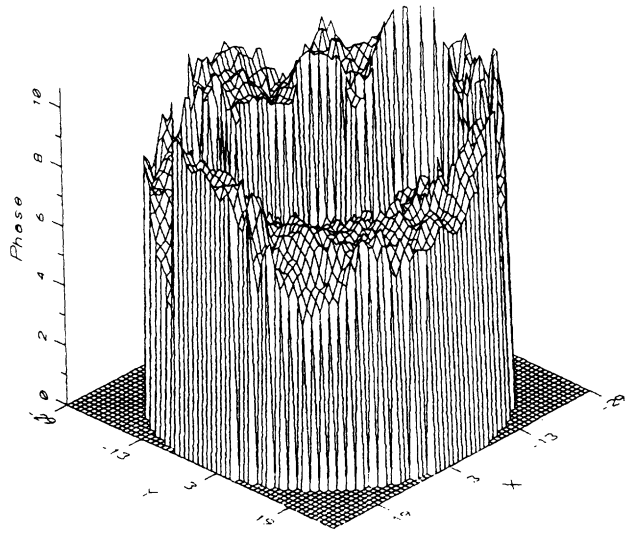

Fig. 2 Surface drawing of a deformed phase wavefront including the overall tilts before phase tailoring

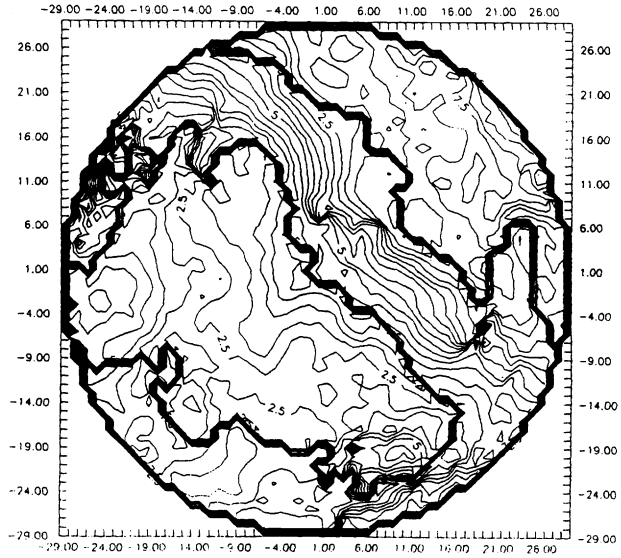

Fig. 3 Topographic drawing of the phase wavefront of Fig. 2

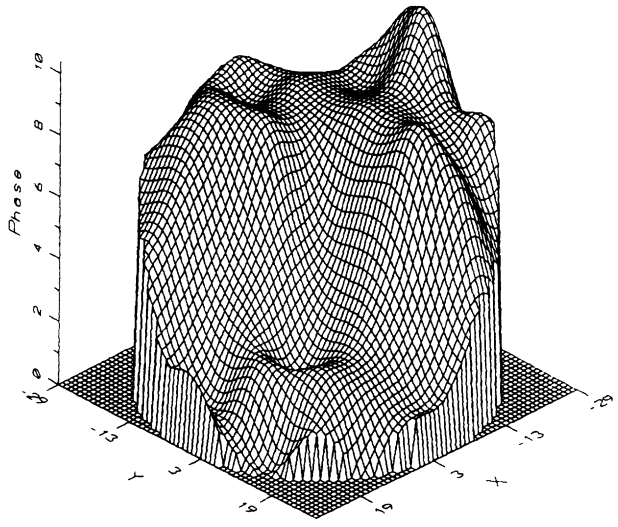

Fig. 4 Surface drawing of the corrected phase wavefront of Fig.2

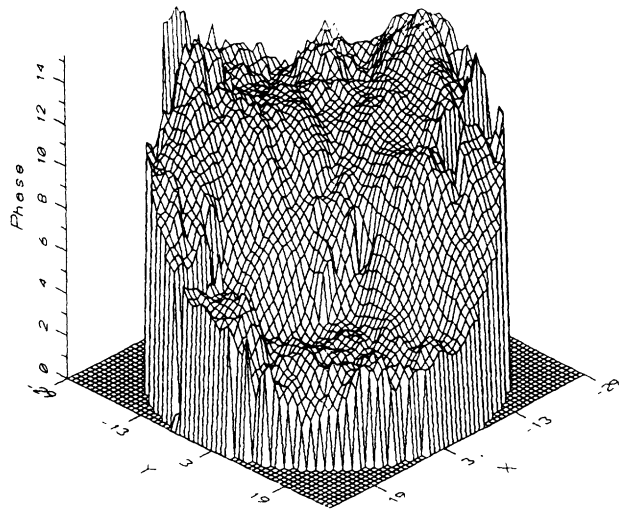

Fig. 5 Surface drawing of the phase wavefront of Fig. 2 after phase tailoring

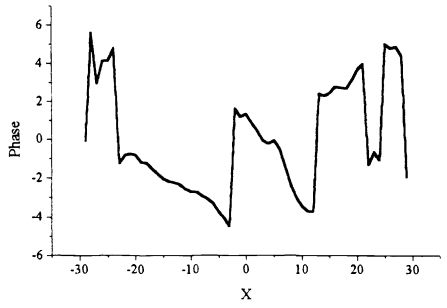

Fig. 6 Cross section of the phase wavefront of Fig. 2 at y-grid point 4

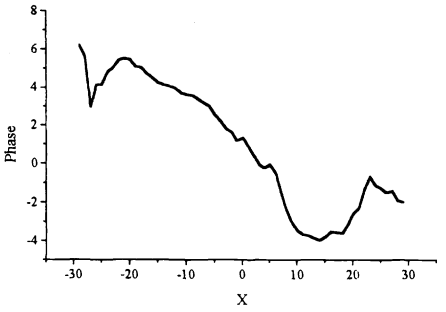

Fig. 7 Cross section of the phase wavefront of Fig. 5 at y-grid point 4

The beam from a beacon may propagate in a stronger turbulent media to reach the HS detector. Figs. 2 and 3 show a disturbed phase wavefront which is calculated from our numerical simulation. Fig. 4 shows the corrected phase after the correction of an AO system of 61 units (with 48 sub-apertures and 61 actuators). It is shown that the correspondence of Figs. 2 and 4 is quite poor although the Strehl ratio (STRCC=0.662) shows the phase compensation should be quite good. We find this abnormality is because the calculated phase has some discontinuities. The calculated phase which is calculated from the inverse trigonometric function is limited within 2π. That is, the discontinuities in the calculated phase are artificial other than practical. In fact, it is impossible that the practical wavefront phase has some discontinuities even it is greatly deformed by the turbulent media. We propose a technique which is called as "phase tailoring" to remove the phase discontinuities. Fig. 5 shows the disturbed phase of Fig. 2 after phase tailoring. Figs. 6 and 7 shows a cross section of the disturbed phase of Figs. 2 and 5, respectively. It is clear that the phase discontinuities are removed after phase tailoring.

Table 6 STRCC in the different turbulent media

Computational conditions: 61 units AO system; others see Table 1.

C_n^2 ($m^{-2/3}$)		10 phase screens			20 phase screens		
	Times	50	100	200	50	100	200
$10^{-14.5}$	OL	0.490	0.481	0.475	0.482	0.477	0.462
	AO	0.855	0.854	0.853	0.857	0.854	0.852
10^{-14}	OL	0.161	0.164	0.164	0.162	0.166	0.160
	AO	0.616	0.614	0.612	0.616	0.611	0.607
$10^{-13.5}$	OL	0.0451	0.0447	0.0448	0.0469	0.0472	0.0451
	AO	0.215	0.211	0.206	0.204	0.202	0.201

For an AO system in static state, it is shown that in the case of stronger turbulence generally 3-4 times iterations are needed to get the best correction effect for one time turbulence realization (see Table 7). It can be seen from Table 7 that the Strehl ratio does not correspond to the phase variance before phase tailoring and the correspondence between the Strehl ratio and phase variance is quite good after phase tailoring. It is seen also that in the case of very weak turbulence the phase tailoring is not needed and 1-2 times iterations are enough to obtain the best correction effect.

In the numerical simulation of laser propagation in a turbulent media, using different random number seed(s) means to produce a different turbulent media although its spectral density for the refractive index fluctuations (von Karman spectrum) and index structure constant are the same. It can be seen from Table 7 that the Strehl ratios and phase variances with and without an AO system are different in different turbulent media.

It is seen from Table 2 that when the turbulence is stronger, the Strehl ratios with and without an AO correction become lower rapidly and about 50 times turbulence realizations are enough for getting usable averaged results.

There are two methods of imaging calculation of the wave field on each sub-aperture. We call them as FFT method and integration method. The former is to utilize the fast Fourier transform (FFT) to calculate the wave propagation equation (5) with n_1=0. The latter is to utilize a direct numerical integration to calculate the Eq.(15) or its equivalent. Eq.(5) can be utilized only under the condition of the parabolic or Fresnel approximation. However, Eq.(15) can be utilized in "any" case.

In order to utilize Eq.(5) and the FFT method, we artificially increase the focus length of each sub-aperture. Table 8 shows that the computational results by utilizing FFT to calculate focusing of wave field on each sub-aperture agree with those by utilizing the integration method excellently. However, the computer time by utilizing FFT method is about 1/20 of that by utilizing integration method.

Table 7 Strehl ratio and phase variance σ_φ^2 without the overall tilt of an AO system

Computational conditions: $\lambda = 0.6328\mu$; L=340m; 37 unit AO system; phase screen grids: 512*512; propagation grids: 128*128; 10 phase screens; 1 time turbulence realization. Condition 1: $C_n^2 = 2.78*10^{-14}(r_0 = 5cm)$; before phase tailoring. Condition 2: $C_n^2 = 2.78*10^{-14}(r_0 = 5cm)$; after phase tailoring. Condition 3: $C_n^2 = 4.455*10^{-15}(r_0 = 15cm)$; before phase tailoring. Condition 4: $C_n^2 = 1.90*10^{-15}(r_0 = 25cm)$; before phase tailoring. Condition 5: $C_n^2 = 2.78*10^{-14}(r_0 = 5cm)$; different phase screens; after phase tailoring.

Condition	1		2		3		4		5	
Iteration times	STRCC	σ_φ^2	STRCC	σ_φ^2	STRCC	σ_φ^2	STRCC	σ_φ^2	STRCC	σ_φ^2
0(OL)	0.469	4.7568	0.469	2.0776	0.835	1.7969	0.922	0.1573	0.338	2.3095
1	0.772	4.8937	0.772	0.5566	0.954	0.0474	0.979	0.0200	0.762	0.3078
2	0.810	5.2581	0.810	0.4695	0.965	0.0345	0.983	0.0146	0.818	0.2256
3	0.813	5.4267	0.813	0.3543	0.965	0.0347	0.983	0.0147	0.818	0.2271
4	0.815	5.4437	0.815	0.2975	0.965	0.0342	0.983	0.0145	0.819	0.2233
5	0.816	5.4341	0.816	0.2652	0.965	0.0343	0.983	0.0145	0.819	0.2229
6	0.815	5.5034	0.815	0.2486	0.965	0.0342	0.983	0.0144	0.819	0.2219
7	0.815	5.4999	0.815	0.2401	0.965	0.0341	0.983	0.0144	0.819	0.2215
8	0.814	5.4735	0.814	0.2359	0.965	0.0341	0.983	0.0143	0.819	0.2211
9	0.814	5.4757	0.814	0.2341	0.965	0.0341	0.983	0.0144	0.819	0.2208
10	0.814	5.4707	0.814	0.2334	0.965	0.0341	0.983	0.0144	0.819	0.2206

In the practical application of an AO system, the system has limited response in all three portions of wavefront detection. reconstruction and correction and the output of compensated phase should be delayed. Practically, this is the topic of dynamic control. We utilize a effective delay time Δt to include this effect in the present stage of numerical simulation of an AO system in static state and think that the main laser beam with the compensated wavefront radiates out after Δt. In this period time, the phase screens move under the actions of lateral wind and/or lateral movements of target and laser source.

Table 8 Comparison of focusing calculations by utilizing FFT and integration method

Computational conditions: iteration times: 4; $C_n^2 = 2.78*10^{-14}(r_0 = 5cm)$; others see Table 7.

Times	OL	FFT	Int.
1	0.338	0.819	0.819
2	0.406	0.827	0.828
3	0.311	0.836	0.836
4	0.268	0.826	0.826
5	0.236	0.828	0.828
10	0.236	0.844	0.845
20	0.221	0.840	0.840
30	0.237	0.839	0.839
40	0.233	0.834	0.834
50	0.245	0.834	0.834

Table 9 Effects of lateral wind speed V on STRCC of AO phase compensation and complete phase conjugation (CPC)

Computational conditions: delay time 4.5ms; 50 times turbulence realizations; others see Table 8.

V(m/s)	OL	AO	CPC
0	0.245	0.834	0.978
2	0.253	0.667	0.673
4	0.254	0.443	0.412
6	0.252	0.322	0.294
8	0.246	0.226	0.241
10	0.252	0.232	0.208
13	0.250	0.204	0.182

The numerical simulation results of laser propagation and a practical AO system with delay time of 4.5ms in different lateral wind speeds are shown in Table 9. The results of open loop (without AO system) and those with complete phase conjugation (CPC) are included as well. It is apparent that as the wind speed increases the AO phase compensation results become worse rapidly. The complete phase conjugation results become worse even more rapidly. In the case that the turbulent media does not move, the complete phase conjugation results is better than those with AO phase compensation.

However, when the wind speed is larger than a certain value (on the condition of Table 9, V>3 m/s), the results with AO phase compensation become better than those with the complete phase conjugation. As the lateral wind speed is further high, the complete phase conjugation results even become worse than those without any phase compensation.

It is concluded that when the AO system has a certain delay time, an AO system with a better phase compensation capability does not mean it will produce a better compensation result. In order to obtain a better AO compensation result, besides improving the phase compensation capability of an AO system such as increasing numbers of sub-apertures and deformable mirror actuators, it is necessary (and might be more important) to decrease the delay time and improve the dynamic control performance of the system.

By the way, we also did the numerical simulation by utilizing filtering method in which an AO system is simplified as a high pass filter. It is shown that the filtering method with a proper band pass can give reasonable results in some cases, but it can not give quantitative results on various conditions even for an AO system in static state. The filtering method is only a rough approximation.

Our numerical simulation including the effects of noise and detection error and dynamic control process is in progress.

ACKOWLEDGEMENT

The authors gratefully acknowledge many helpful discussions with Academician Wenhan Jiang.

REFERENCES

1. R.K.Tyson, *Principles of Adaptive Optics*, Academic Press, New York, 1991.
2. Wenhan Jiang and Huagui Li, "Hartmann-Shack wavefront sensing and wavefront control algorithm", *Proc. SPIE* Vol.**1271**, pp. 82-93, 1990.
3. C.Boyer, V.Michon and G.Rousset, "Adaptive optics: Interaction matrix measurements and real time control algorithms for the COME-ON project," *Proc. SPIE*, Vol.**1237**, pp. 406-423, 1990.
4. R.J.Noll, "Zernike polynomials and atmospheric turbulence," *J. Opt. Soc. Am.* **66**, pp. 207-211, 1976.
5. J.A.Fleck,Jr., J. R. Morris, and M. D. Feit, "Time-dependent propagation of high energy laser beams through the atmosphere", *Appl. Phys.* **10**, pp. 129-160, 1976.
6. J.M.Martin and S.M.Flatte, "Intensity images and statistics from numerical simulation of wave propagation in 3-D random media", *Appl. Opt.* **27**, pp. 2111-2126, 1988.
7. B.M.Welsh and C.S.Gardner, "Effects of turbulence-induced anisoplanatism on the imaging performance of adaptive-astronomical telescopes using laser guide stars," *J. Opt. Soc. Am.* **A8**, pp. 69-80, 1991.
8. R.R.Parenti and R.J.Sasiela, "Laser-guide-star systems for astronomical applications," *J. Opt. Soc. Am.* **A11**, pp. 288-309, 1994.
9. P.B.Ulrich and L.E.Wilson (ed.), Propagation of High-Energy Laser Beams through the Earth's Atmosphere, *Proc. SPIE* Vol.**1221,** 1990; P.B.Ulrich and L.E.Wilson (ed.), Propagation of High- Energy Laser Beams through the Earth's Atmosphere II, *Proc. SPIE* Vol.**1408**, 1991.
10. R.V.Digumarthi, N.G.Metha and R. M. Blankinship, "Effects of a realistic adaptive optics system on the atmospheric propagation of a high energy laser beam", *Proc. SPIE* Vol.**1221**, pp. 157-165, 1990.
11. C.A.Primmerman, T.R.Price, R.A.Humphreys, B.G.Zollars, H.T.Barclay and J.Herrman, "Atmospheric-compensation experiments in strong-scintillation conditions," *Appl. Opt.* **34**, pp. 2081-2088, 1995.